Graphite Oxide and Aromatic Amines: Size Matters

Konstantinos Spyrou, Matteo Calvaresi, Evmorfia K. Diamanti, Theodoros Tsoufis, Dimitrios Gournis, Petra Rudolf,* and Francesco Zerbetto**

Dedicated to Prof. Maurizio Prato on the occasion of his 60th birthday.

Experimental and theoretical studies are performed in order to illuminate, for first time, the intercalation mechanism of polycyclic aromatic molecules into graphite oxide. Two representative molecules of this family, aniline and naphthalene amine are investigated. After intercalation, aniline molecules prefer to covalently connect to the graphene oxide matrix via chemical grafting, while napthalene amine molecules bind with the graphene oxide surface through π–π interactions. The presence of intercalated aromatic molecules between the graphene oxide layers is demonstrated by X-ray diffraction, while the type of interaction between graphene oxide and polycyclic organic molecules is elucidated by X-ray photoelectron spectroscopy. Combined quantum mechanical and molecular mechanical calculations describe the intercalation mechanism and the aniline grafting, rationalizing the experimental data. The present work opens new perspectives for the interaction of various aromatic molecules with graphite oxide and the so-called "intercalation chemistry".

1. Introduction

Graphene is a one-atom thick layer of sp^2 hybridized carbon atoms, tightly packed in a hexagonal crystal lattice and constitutes the main basic building block of other graphitic nanostructures like graphite, fullerenes and nanotubes. The extraordinary/unusual properties of graphene[1,2] promise well for numerous, very different applications in electronics and spintronics, but also as reinforcement in polymer composites, constituent of composite materials or active element in sensors.[3–10] To realize this potential, efficient approaches for the production of large quantities of graphene are needed; currently one of the most promising is the chemical exfoliation of graphite passing the oxidation of the graphene sheets in order to form graphene oxide.[8,11,12] Graphene or graphite oxide (GO) is a layered material achieved through strong oxidation of graphite.[13–15] GO is characterized by the presence of oxygen–containing moieties, mostly hydroxyl and epoxy groups on the basal plane, and carboxyl groups prevalently at the edges of the carbon sheets. These groups convert hydrophobic graphite into highly soluble graphite oxide in several polar and non-polar solvents, including water.[16,17] By now the attachment of functional groups is exploited by the well-established intercalation chemistry[18–20] leading to graphene-based hybrid materials for electrochemical sensors and biosensors or fillers in composite materials for engineering applications, supercapacitors, energy storage and environmental applications.[8,21–26]

Although the adsorption of organic molecules on carbon surfaces has been studied extensively for many years[27–31] no mechanism for covalent or non-covalent functionalization of graphene sheets through chemical grafting or π–π interactions respectively, using aromatic molecules has been reported up to now. Studies on carbon nanotubes have shown strong adsorption affinity with many organic contaminants including polycyclic aromatic hydrocarbons[23,32–35] where the high adsorptive interactions of carbon nanotubes and aromatic molecules derive from the π–π electron donor–acceptor interaction between the conjugated core of the molecules (donors) and the carbon nanotubes (acceptors).[23,36,37] In this work, we demonstrate for the first time the mechanism, by which two aromatic molecules, aniline and naphthalene amine, interact with the graphite oxide matrix and form new intercalated hybrid nanostructures. The structure and properties of this new class of materials may lead to potentially promising applications in water treatment, catalysis, solid state gas sensors, and energy storage devices.

Dr. K. Spyrou, Dr. T. Tsoufis, Prof. P. Rudolf
Zernike Institute for Advanced Materials
University of Groningen
Nijenborgh 4, 9747, AG, Groningen
(The Netherlands)
E-mail: p.rudolf@rug.nl
Dr. M. Calvaresi, Prof. F. Zerbetto
Dipartimento di Chimica "G. Ciamician"
Alma Mater Studiorum – Università di Bologna
Via F. Selmi 2, I-40126, Bologna, Italy
E-mail: francesco.zerbetto@unibo.it
Dr. E. K. Diamanti, Prof. D. Gournis
Department of Materials Science & Engineering
University of Ioannina
45110, Ioannina, Greece
E-mail: dgourni@cc.uoi.gr

DOI: 10.1002/adfm.201402622

2. Results and Discussion

X-ray diffraction (XRD) data were collected to investigate the intercalation of aniline and naphthalene amine molecules into the interlayer space of graphite oxide. **Figure 1** displays the XRD pattern of graphite oxide (GO), and of graphite oxide after mixing with aniline (GO_A) and naphthalene amine

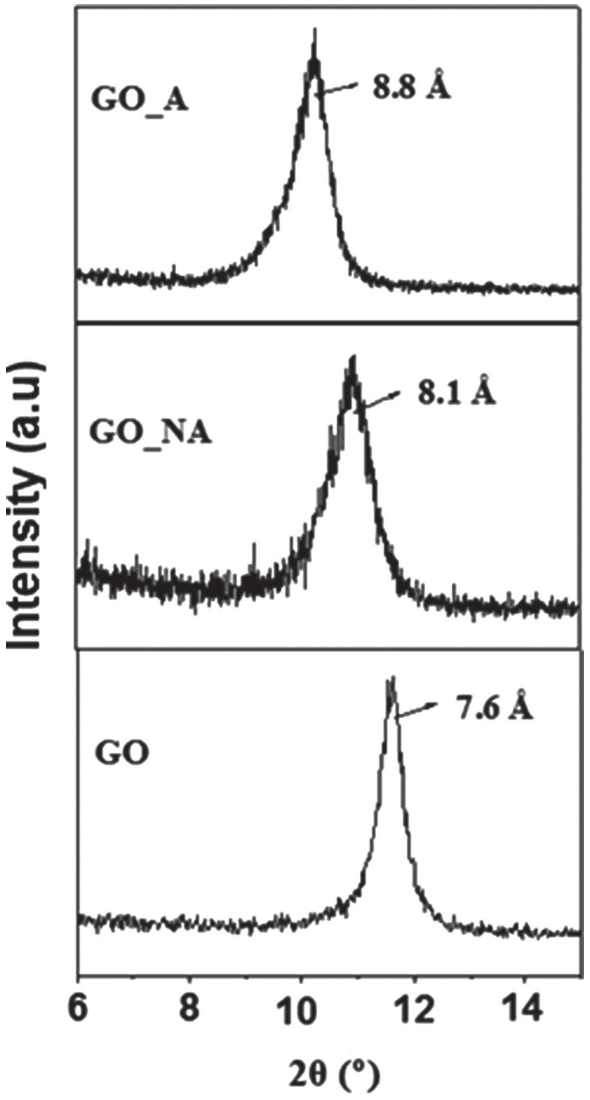

Figure 1. Comparative XRD data of graphite oxide (GO (for details see text)), graphite oxide intercalated with aniline (GO_A) and graphite oxide intercalated with naphthalene amine (GO_NA).

(GO_NA). The position of the diffraction peak of graphene oxide corresponds to a d_{001} spacing of 7.6 ± 0.3 Å (the 7.6 Å distance is the sum of the thickness of a GO layer, which is 6.1 Å, plus a monolayer of adsorbed water molecules), which agrees with literature values relative to swelling when GO is brought in contact with water and dried again.[37] We observe a shift to lower angles of the diffraction peak for both the GO_A and GO_NA hybrid nanostructures as compared to GO, indicating a larger distance between the graphene layers and therefore pointing to the successful intercalation of the aromatic species. In detail, for GO_A the basal d_{001} spacing increased to 8.6 ± 0.3 Å, while for GO_NA the d_{001} spacing amounted to 8.1 ± 0.3 Å. Taking into account the thickness of GO layer (6.1 Å),[38] we estimated the additional opening of the graphene oxide layers after the insertion of the aromatic amines: in the case of aniline intercalation this additional opening amounts to ~2.5 Å, while for naphthalene amine intercalation it is ≈2.0 Å.

Insight into the type of interaction between the aromatic molecules and the graphene oxide sheets can be gained from X-ray photoelectron spectroscopy (XPS). **Figure 2** (left panel) shows the C 1s core level region of the XPS spectrum of GO, displaying four contributions at 285.0 eV, 285.9 eV, 287.2 eV and 288.3 eV binding energy. The peak at 285.0 eV originates from carbon-carbon bonds of the hexagonal lattice and accounts for 22.8% of the total carbon intensity. The contribution at 287.2 eV is due to the C = O (carbonyl) as well C–O–C (epoxy) functional groups and accounts for 46.1% of the total carbon intensity. Two peaks centered at 285.9 eV and 288.3 eV arise from the C–O and C(O)O bonds, representing 17.3% and 13.7% of the total carbon 1s peak intensity, respectively. After the intercalation of aniline and naphthalene amine into the GO galleries, the chemical composition of the resulting hybrid nanostructures changed in comparison with the starting material. In the C 1s spectra of GO_A and GO_NA (shown in the right panel of Figure 2) we observe a significant increase of the intensity of the peak due to C–C bonds centered at 285.0 eV. More specifically, the relative intensity of this contribution rises to 41.8% for GO_A and to 46.4% in the case of GO_NA, demonstrating the presence of a carbonaceous material co-existing with the GO lattice. The peaks at 285.9 eV (12.7%) for GO_A and 286.0 eV (11.1%) for GO_NA hybrids correspond to the C-O bonds of the GO lattice as well from the C–N functional groups of the aromatic species. Finally, in the case of GO_A two more peaks at 287.1 eV (37.1%) and 288.3 eV (8.4%) reveal the presence of carbonyl and carboxyl groups, respectively in our final material. On the other hand, for GO_NA in addition to the peaks corresponding to the carbonyl groups at 287.1 eV (34.5%) and to the carboxyl groups at 288.6 eV (6.3%) we clearly observe the existence of the shake-up satellite peaks from the π–π transitions of the benzene rings and the graphite sheets at 290.7 eV,[39] in contrast with GO_A, where this peak is suppressed. We can conclude that naphthalene amine prefers to bind between the graphene oxide sheets via π–π interactions, while aniline chemically binds to the functional groups of GO.[16,40] The ratio of the total intensities of the carbon 1s to oxygen 1s photoemission lines for GO, GO_A and GO_NA is presented in **Table 1**. This ratio increased after intercalation of aniline from 1.62 to 2.12 and after intercalation of naphthalene amine from 1.62 to 2.91.

Additional significant information on the type of interaction of aniline and naphthalene amine with the graphene oxide sheets comes from the N 1s core level region of the photoelectron spectra of GO_A and GO_NA (shown in **Figure 3**). The spectrum of both the aniline and the naphthalene amine intercalated structures can be deconvoluted into two main peaks placed at ≈399.5 eV and ≈400.8 eV binding energy, which correspond to amine groups and protonated amines of the aromatic species, respectively.[41] For GO_A and GO_NA we see clear differences stemming from how aniline and naphthalene amine interact with the graphene oxide layers. In the case of GO_A, the photoelectron peak attributed to amine groups of aniline is shifted to lower binding energies (398.8 eV), pointing to the creation of a chemical bond with the functional groups of GO (C–N–C bond).[42–44] Taking into account the size of aniline and combining the informing about the covalent bonding with the XRD data, we conclude that these molecules must have an inclined orientation when inserted between the graphene oxide

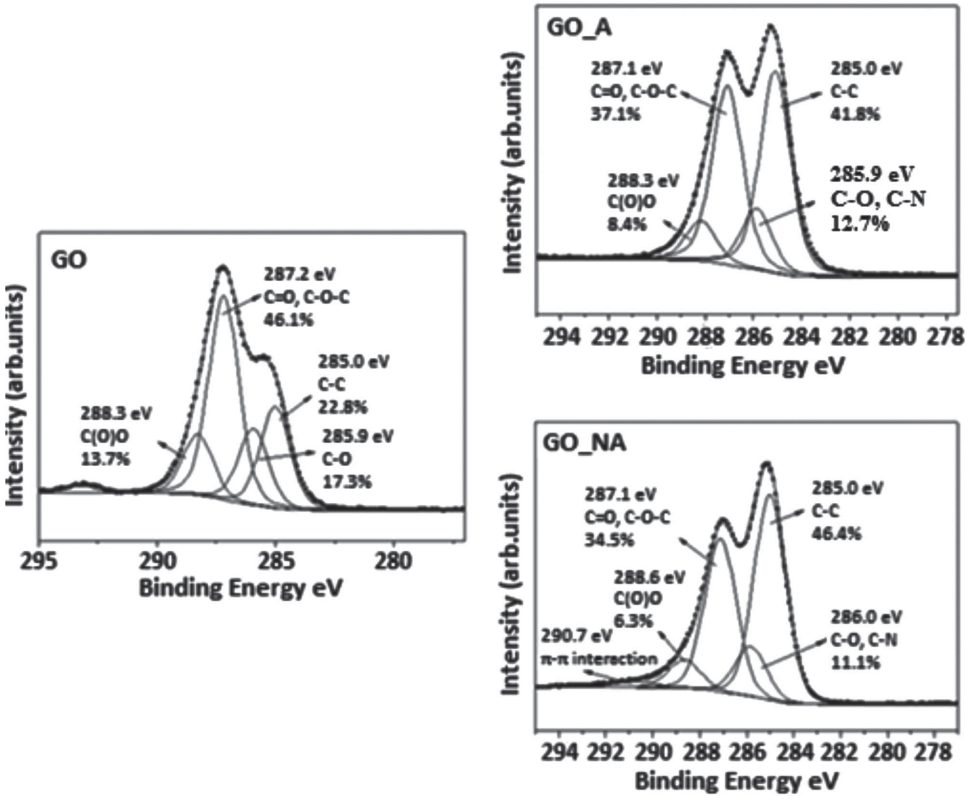

Figure 2. X-ray photoelectron spectra of the C 1s core level region of graphite oxide (GO), graphite oxide intercalated with aniline (GO_A) and graphite oxide intercalated with naphthalene amine (GO_NA).

sheets. For GO_NA we do not observed any significant change on the N 1s XPS spectrum with respect to that of a drop cast film of naphthalene amine (presented in the right top panel of Figure 3 right). This matches with the interpretation of the C 1s XPS spectrum of GO_NA because in the case of π–π interactions the amine functional groups do not participate in any bonding but are present as free groups inside the graphene oxide galleries.

To further confirm the exact type of interaction between aniline and naphthalene amine species with the graphene oxide lattice during the intercalation process, two additional experiments were performed, that is, we repeated the same intercalation experiments in an acidic environment (pH = 4) for both aniline and naphthalene amine. In the case of aniline, at acidic pH (pH = 4) no intercalation occurs as revealed by XRD measurements (**Figure 4**b). This seems to be reasonable if we consider that covalent bonding of aniline is taking place through chemical grafting of the amine groups of aniline with the functional groups of GO, a reaction that happens only at basic pH where the amine groups are not protonated.[16] On the other hand XRD measurements reveal intercalation of naphthalene amine in the GO interlayerspace under acidic pH (pH = 4) (Figure 4c) due to π–π interactions of the naphthalene amine aromatic rings with the graphene oxide sheets. In fact, these interactions do not depend on the pH of the solution where the intercalation take place.[16] The increase of the d_{001} spacing of GO for naphthalene amine and the invariability of the first order peak of GO for aniline are a further confirmation for the type of binding of these molecules with GO surfaces. It is noteworthy that two other members of aromatic amines with additional number of aromatic rings like anthracene amine (ANA) and pyrene amine (PA) exhibit a behavior similar to that of NA when attached on the surface of graphene oxide, as demonstrated by X-ray diffraction and X-ray photoelectron spectroscopy techniques (see Supporting Information).

Table 1. Ratio of the total intensities of the carbon 1s to oxygen 1 s photoemission lines for GO, GO_A, and GO_NA.

GO	GO_A	GO_NA
1.62 ± 0.03	2.12 ± 0.06	2.91 ± 0.06

Recent structural models of GO describe it as graphene decorated with epoxy (1,2-ether) and hydroxyl functional groups spread non-stoichiometrically across the basal planes of graphite.[17,45,46] The grafting of amine moieties to GO can be explained by the nucleophilic reaction of amine with the basal plane of GO that can proceed via two different mechanisms: (i) a ring opening reaction of the epoxy groups of GO; (ii) a nucleophilic reaction with the Cα of a hydroxyl group.

The energy profiles of the two mechanisms were studied by QM/MM calculations. **Figure 5** and **Table 2** show that the reaction with the C atom near to a hydroxyl group, Cα, has a lower energy barrier than the direct reaction with the epoxide group. More interestingly, E_a for the reaction of aniline has a barrier that is ≈3 kcal mol^{-1} lower than for the similar reaction

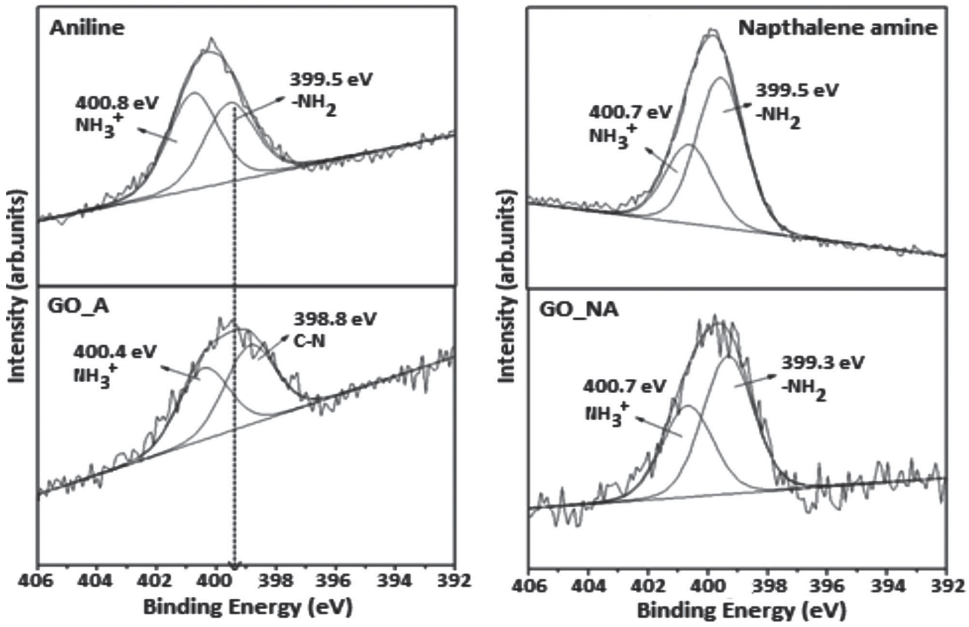

Figure 3. X-ray photoelectron spectra of the nitrogen 1s core level region of aniline, graphite oxide intercalated with aniline (GO_A), and graphite oxide intercalated with naphthalene amine (GO_NA). The spectrum of a drop cast film of naphthalene amine is also shown for comparison.

of naphthalene amine. Simple Arrhenius law considerations, at room temperature, make the ratio of the reaction rates for the two molecules 160:1 in favor of aniline.

Compared to naphthalene amine, two factors determine the lower E_a of aniline: i) its higher nucleophilicity, and ii) the weaker interaction between its aromatic ring and GO. Delocalization onto the naphthalene ring of the lone pair of nitrogen makes naphthalene amine less basic and less nucleophilic than aniline. Accordingly, the calculations show that the structure of the transition state of the reaction with aniline is "earlier"

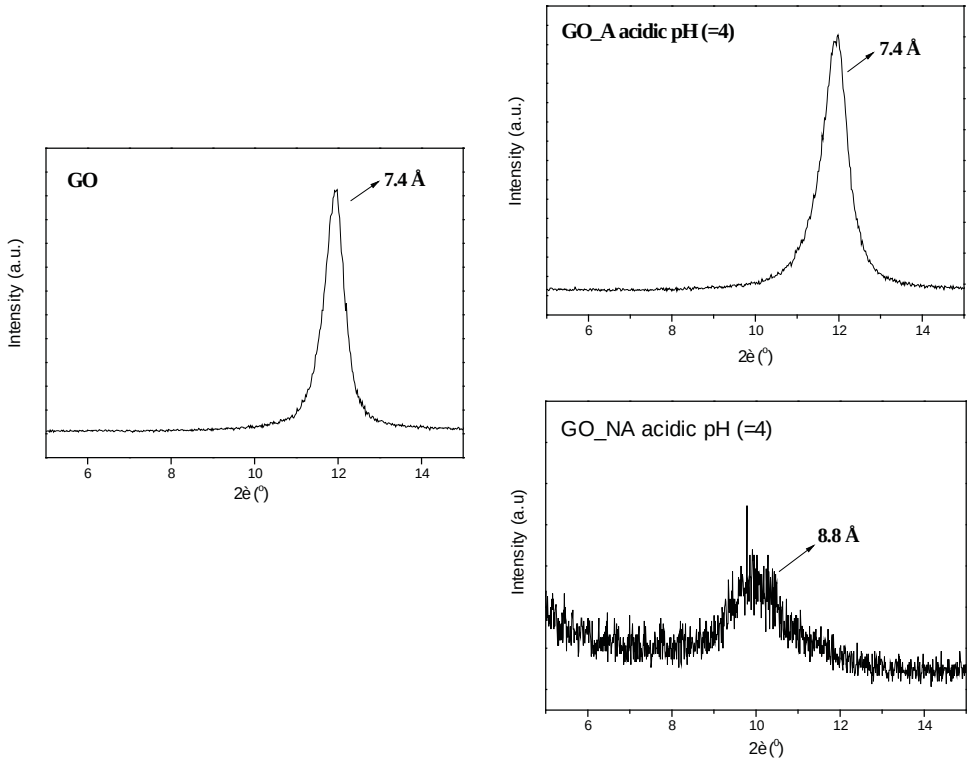

Figure 4. X-ray diffraction measurements (XRD) of pristine graphite oxide (GO) and aniline intercalated graphite oxide (GO_A) and naphthalene amine intercalated graphite oxide (GO_NA) at acidic pH (pH = 4).

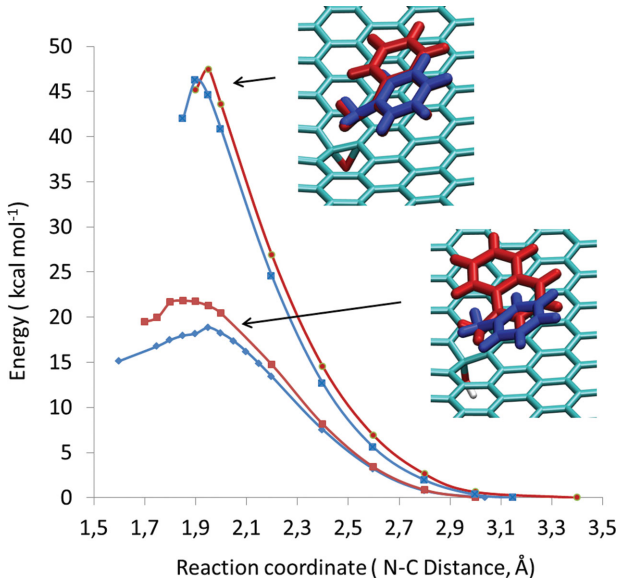

Figure 5. Reaction coordinates for the opening of an epoxy group of GO (higher barrier) and the reaction with the C_α of a hydroxyl group (lower barrier) by naphthalene amine (red) and aniline (blue).

(N–C distance 1.95 Å) than the corresponding one for the NA attack (N–C distance 1.85 Å). In practice, the aniline lone pair reaches further and is therefore more nucleophilic. Moreover, in the pre-reactive complex, both aromatic amines lie parallel to the basal plane of GO. This is confirmed by geometry optimization of the π–π complexes formed by the aromatic rings of the amine and the basal plane of GO. The interaction energy of naphthalene amine is greater than the interaction energy of aniline (9.3 kcal mol^{-1} vs 4.4 kcal mol^{-1}, **Table 3**).

In the transition state of the reactions of the aromatic amines with GO, they must assume a tilted position with respect to the graphene oxide plane, which slackens the π–π interactions and loses part of the stabilizing interactions. For naphthalene amine this energy cost is greater because of the larger interaction of the naphthalene moiety compared to that of the phenyl ring.

Table 3 can also explain the experimental behavior of the protonated amines. Experimentally, in an acidic environment (pH = 4), no grafting or intercalation occurs for aniline. The calculations show that the interaction of protonated aniline with GO is endothermic (+2.7 kcal mol^{-1}). Protonated aniline, therefore, prefers to remain in the water solution. In the same experimental conditions intercalation of naphthalene amine in GO still occurs. The value of the interaction between naphthalene amine and GO, even if lower in the protonated state (4.4 kcal mol^{-1} vs 9.3 kcal mol^{-1}), is still exothermic. The different behavior between aniline and naphthalene amine can

Table 2. QM/MM M06–2X/6–31G*:UFF energy barriers, E_a, for the opening of an epoxy group of GO and for the reaction with the C_α of a hydroxyl group by naphthalene amine and aniline.

	Epoxy (E_a in kcal mol^{-1})	Hydroxyl (E_a in kcal mol^{-1})
Aniline	46.3	18.8
Naphthalene amine	47.5	21.8

Table 3. Interaction free energy for the complexes between GO and aniline or naphthalene amine. Both protonated and non-protonated amines are considered.

	Non-protonated amine (ΔG in kcal mol^{-1})	Protonated amine (ΔG in kcal mol^{-1})
Aniline	–4.4	2.7
Naphthalene amine	–9.3	–4.4

be readily explained by the larger π–π interaction of the naphthalene group with GO with respect to the phenyl ring, which compensates the entropic cost of the intercalation and of the (partial) desolvation of the protonated amine when it enters between GO sheets.

3. Conclusions

In this study, experimental and theoretical approaches were combined to demonstrate the successful intercalation of common organic polycyclic aromatic compounds between the layers of graphite oxide (GO), and to examine in detail the mechanism by which each molecule interacts with the graphene oxide surface. We prove that the type of interaction for aniline and naphthalene amine with the graphene oxide layers differs according to the size of the aromatic molecules. More specifically we show that aniline covalent binds with the graphite oxide matrix through chemical grafting, while naphthalene amine prefers to adsorb on the surface of graphene oxide by π–π interactions. This novel class of hybrid materials opens new horizons in intercalation chemistry and may drive potential applications in electronics, energy storage and environmental remediation. Aniline and its derivatives are considered highly toxic agents which are absorbed well by inhalation and through the skin. They are responsible for short-term and chronic effects such as irritation and congestion of the lung, sensitisation, genotoxicity and carcinogenesis.[47] As a consequence the creation of a material capable of absorbing high amounts of aniline is of crucial importance. GO can immobilize high amounts of aniline through covalent bonding and stabilizes the molecules on the graphene surface. The adsorption of aniline on GO for water and air purification should therefore be investigated.

4. Experimental Section

Preparation of Graphite Oxide (GO): 10 g of powdered graphite (purum, powder ≤0.2 mm; Fluka) were added to a mixture of concentrated sulphuric acid (400 mL, 95–97 wt%) and nitric acid (200 mL, 65 wt%) while cooling in an ice-water bath. Potassium chlorate powder (200 g, purum, >98.0%; Fluka) was added to the mixture in small portions while stirring and cooling. The reactions were quenched after 18 h by pouring the mixture into distilled water and the oxidation product was washed until the pH reached the value 6. The sample was then dried at room temperature.

Intercalation of Aniline in GO (GO_A): A sample of 100 mg of graphite oxide was dispersed in 100 mL of water (H_2O) and the solution was stirred for 24 h at ambient conditions. Afterwards we increased the pH of the solution to 10 by adding (dropwise) NaOH 0.5 M. Then 0.3 mL of aniline were added (dropwise) to 20 mL of H_2O and the solution left

stirring for 24 while being mildly heated at 40 °C. Finally the solution of aniline was added to the one of GO. After stirring for 48 h, the GO_A aggregates were washed with water three times, separated by centrifugation and air-dried by spreading on glass plates.

Intercalation of Naphthaleneamine in GO (GO_NA): In a similar experiment/procedure, 100 mg of graphite oxide were dispersed in 100 mL of H_2O and the mixture was stirred for 24 h at ambient conditions. The pH was increased to 10 by adding (dropwise) NaOH 0.5 M. A solution of naphthaleneamine (300 mg) in H_2O (20 mL) was then added dropwise to the GO suspension and the mixture was stirred for 24 h at ambient conditions. The final solution was washed with H_2O three times separated by centrifugation and air-dried by spreading on glass plates.

X-Ray Photoelectron Spectroscopy (XPS): X-ray photoelectron spectroscopy (XPS) data were collected using an SSX-100 (Surface Science Instruments) spectrometer equipped with a monochromatic Al Kα X-ray source ($h\nu$ = 1486.6 eV). The photoelectron take-off angle was 37° with respect to the surface normal and the energy resolution was set to 1.2 eV to minimize data acquisition time. All binding energies were referenced to the C 1s core level line[48] of the C–C bond at 285.0 eV and are given ±0.1 eV. Spectral analysis included a Shirley background subtraction and peak separation using mixed Gaussian-Lorentzian functions in a least-squares curve-fitting program (Winspec) developed in the LISE laboratory of the University of Namur, Belgium. For the N 1s line we employed a linear background subtraction due to low peak intensity, which does not allow for Shirley background subtraction. The photoemission peak areas of each element, used to estimate the amount of each species within the probed volume, were normalized by the sensitivity factors of each element tabulated for the spectrometer used. The substrates were evaporated on freshly gold films supported on mica; four points were measured on each sample in order to guarantee the reproducibility of the results.

X-Ray Diffraction (XRD): XRD patterns of thin films were collected using a Philips PANanlyticalX'Pert MRD diffractometer with a Cu Kα (λ = 1.5418 Å) radiation source (40 kV, 40 mA), a 0.25° divergent slit and a 0.125° antiscattering slit. The reflectivity patterns were recorded in the 2-Theta (2θ) range from 0.5 to 30° with 0.02° steps and a counting time of 15 s per step. For the preparation of the films, aqueous suspensions of the samples were deposited on silicon substrates, and left to dry at ambient conditions.

Computational Details: All calculations were carried out using the combined quantum mechanical and molecular mechanical (QM/MM) method in the ONIOM formalism, as implemented within the Gaussian 09 program suite.[49] The coupled QM/MM method adopted here is a two-layer ONIOM scheme, where the reactive region is treated at DFT level using the density functional M062X (a functional able to account for π–π interactions).[50] The remaining region is treated using the UFF force field.[51] 6–31G* basis set[52] was used for the QM region. The global potential can be referred as M06–2X/6–31G*:UFF potential. The Polarized Continuum Model[53] was used to mimic the aqueous environment where the reaction/intercalation takes place. QM/MM frequency calculations on the whole system were carried out to determine the nature of the critical points identified on the potential energy surface PES and to calculate Gibbs free energy corrections at standard ambient temperature and pressure.

Supporting Information

Supporting Information is available from the Wiley Online Library or from the author.

Acknowledgements

This work was performed within "Top Research School" program of the Zernike Institute for Advanced Materials under the Bonus Incentive Scheme (BIS) of the Netherlands' Ministry of Education, Science, and Culture and received additional support from the Foundation for Fundamental Research on Matter (FOM), part of the Netherlands Organisation for Scientific Research (NWO). This work was also co-financed by the European Union (European Social Fund – ESF) and Greek national funds through the Operational Program "Education and Lifelong Learning" of the National Strategic Reference Framework (NSRF) – Research Funding Program: THALES. Investing in knowledge society through the European Social Fund.

Received: August 3, 2014
Revised: September 26, 2014
Published online: November 12, 2014

[1] K. S. Novoselov, A. K. Geim, S. V. Morozov, D. Jiang, Y. Zhang, S. V. Dubonos, I. V. Grigorieva, A. A. Firsov, *Science* **2004**, *306*, 666.
[2] A. K. Geim, K. S. Novoselov, *Nat. Mater.* **2007**, *6*, 183.
[3] J. Wu, W. Pisula, K. Müllen, *Chem. Rev.* **2007**, *107*, 718.
[4] A. A. Balandin, S. Ghosh, W. Bao, I. Calizo, D. Teweldebrhan, F. Miao, C. N. Lau, *Nano Lett.* **2008**, *8*, 902.
[5] K. S. Kim, Y. Zhao, H. Jang, S. Y. Lee, J. M. Kim, K. S. Kim, J.-H. Ahn, P. Kim, J.-Y. Choi, B. H. Hong, *Nature* **2009**, *457*, 706.
[6] S. Bae, H. Kim, Y. Lee, X. Xu, J. S. Park, Y. Zheng, J. Balakrishnan, T. Lei, H. Ri Kim, Y. I. Song, Y. J. Kim, K. S. Kim, B. O'zyilmaz, J. H. Ahn, B. H. Hong, S. Iijima, *Nat. Nanotechnol.* **2010**, *5*, 574.
[7] N. Tombros, C. Jozsa, M. Popinciuc, H. T. Jonkman, B. J. Van Wees, *Nature* **2007**, *448*, 571.
[8] S. Stankovich, D. A. Dikin, G. H. B. Dommett, K. M. Kohlhaas, E. J. Zimney, E. A. Stach, R. D. Piner, S. T. Nguyen, R. S. Ruoff, *Nature* **2006**, *442*, 282.
[9] L. Brey, H. A. Fertig, *Phys. Rev. B* **2006**, *73*.
[10] F. Schedin, A. K. Geim, S. V. Morozov, E. W. Hill, P. Blake, M. I. Katsnelson, K. S. Novoselov, *Nat. Mater.* **2007**, *6*, 652.
[11] R. Verdejo, F. Barroso-Bujans, M. A. Rodriguez-Perez, J. A. De Saja, M. A. Lopez-Manchado, *J. Mater. Chem.* **2008**, *18*, 2221.
[12] M. Segal, *Nat. Nanotechnol.* **2009**, *4*, 612.
[13] B. C. Brodie, *Ann. Chim. Phys.* **1860**, *59*, 466.
[14] L. Staudenmaier, *Ber. Deut. Chem. Ges.* **1898**, *31*, 1481.
[15] W. S. Hummers Jr, R. E. Offeman, *J. Am. Chem. Soc.* **1958**, *80*, 1339.
[16] A. B. Bourlinos, D. Gournis, D. Petridis, T. Szabo, A. Szeri, I. Dekany, *Langmuir* **2003**, *19*, 6050.
[17] D. R. Dreyer, S. Park, C. W. Bielawski, R. S. Ruoff, *Chem. Soc. Rev.* **2010**, *39*, 228.
[18] R. Bissessur, P. K. Y. Liu, S. F. Scully, *Synth. Met.* **2006**, *156*, 1023.
[19] N. Meng, S. Q. Zhang, N. L. Zhou, J. Shen, *Nanotechnology* **2010**, *21*.
[20] P. Hagenmuller, *J. Phys. Chem. Solids* **1998**, *59*, 503.
[21] Y. Shao, J. Wang, H. Wu, J. Liu, I. A. Aksay, Y. Lin, *Electroanalysis* **2010**, *22*, 1027.
[22] Y. Wang, Z. Shi, Y. Huang, Y. Ma, C. Wang, M. Chen, Y. Chen, *J. Phys. Chem. C* **2009**, *113*, 13103.
[23] W. Chen, L. Duan, D. Zhu, *Environ. Sci. Technol.* **2007**, *41*, 8295.
[24] L. Wang, K. Lee, Y. Y. Sun, M. Lucking, Z. Chen, J. J. Zhao, S. B. Zhang, *ACS Nano* **2009**, *3*, 2995.
[25] J. Guo, R. Wang, W. W. Tjiu, J. Pan, T. Liu, *J. Hazardous Materi.* **2012**, *225–226*, 63.
[26] Z. Jin, J. R. Lomeda, B. K. Price, W. Lu, Y. Zhu, J. M. Tour, *Chem. Mater.* **2009**, *21*, 3045.
[27] D. Zhu, J. J. Pignatello, *Environ. Sci. Technol.* **2005**, *39*, 2033.
[28] Y. Xu, H. Bai, G. Lu, C. Li, G. Shi, *J. Am. Chem. Soc.* **2008**, *130*, 5856.
[29] A. Rochefort, J. D. Wuest, *Langmuir* **2009**, *25*, 210.
[30] M. Calvaresi, M. Quintana, P. Rudolf, F. Zerbetto, M. Prato, *ChemPhysChem* **2013**, *14*, 3447.
[31] a) M. Quintana, M. Grzelczak, K. Spyrou, M. Calvaresi, S. Bals, B. Kooi, G. Van Tendeloo, P. Rudolf, F. Zerbetto, M. Prato, *J. Am. Chem. Soc.* **2012**, *134*, 13310; b) V. León, A. M. Rodriguez, P. Prieto, M. Prato, E. Vázquez, *ACS Nano* **2014**, *8*, 563.

[32] K. Yang, L. Zhu, B. Xing, *Environ. Sci. Technol.* **2006**, *40*, 1855.
[33] R. J. Chen, Y. Zhang, D. Wang, H. Dai, *J. Am. Chem. Soc.* **2001**, *123*, 3838.
[34] N. Nakayama-Ratchford, S. Bangsaruntip, X. Sun, K. Welsher, H. Dai, *J. Am. Chem. Soc.* **2007**, *129*, 2448.
[35] N. Nakashima, Y. Tomonari, H. Murakami, *Chem. Lett.* **2002**, 638.
[36] W. Plank, R. Pfeiffer, C. Schaman, H. Kuzmany, M. Calvaresi, F. Zerbetto, J. Meyer, *ACS Nano* **2010**, *4*, 4515.
[37] X. Liu, H. Kuzmany, P. Ayala, M. Calvaresi, F. Zerbetto, T. Pichler, *Adv. Funct. Mater.* **2012**, *22*, 3202.
[38] I. Dekany, R. Kruger-Grasser, A. Weiss, *Colloid Polym. Sci.* **1998**, *276*, 570.
[39] S. Biniak, G. Szymański, J. Siedlewski, A. Eświatkoski, *Carbon* **1997**, *35*, 1799.
[40] R. Y. N. Gengler, A. Veligura, A. Enotiadis, E. K. Diamanti, D. Gournis, C. Jozsa, B. J. van Wees, P. Rudolf, *Small* **2010**, *6*, 35.
[41] P. R. Moses, L. M. Wier, J. C. Lennox, H. O. Finklea, J. R. Lenhard, R. W. Murray, *Anal. Chem.* **1978**, *50*, 576.
[42] A. M. Ektessabi, S. Hakamata, *Thin Solid Films* **2000**, *377–378*, 621.
[43] J. W. Shin, J. P. Jeun, P. H. Kang, *Macromol. Res.* **2010**, *18*, 227.
[44] M. Herrera-Alonso, A. A. Abdala, M. J. McAllister, I. A. Aksay, R. K. Prud'homme, *Langmuir* **2007**, *23*, 10644.
[45] H. He, T. Riedl, A. Lerf, J. Klinowski, *J. Phys. Chem.* **1996**, *100*, 19954.
[46] A. Lerf, H. He, M. Forster, J. Klinowski, *J. Phys. Chem. B* **1998**, *102*, 4477.
[47] European Commision, Health & Consumer Protection Directorate-General, Scientific Committee on Toxicity, Ecotoxicity and the Environment (CSTEE), Opinion on the results of the Risk Assessment of Aniline, Human Health part (CAS N° : 62–53–3 EINECS N° : 200–539–3), C2/GF/csteeop/Aniline/01042003 D(03), http://ec.europa.eu/food/fs/sc/sct/out183_en.pdf
[48] M. Lotya, Y. Hernandez, P. J. King, R. J. Smith, V. Nicolosi, L. S. Karlsson, F. M. Blighe, S. De, Z. Wang, I. T. McGovern, G. S. Duesberg, J. N. Coleman, *J. Am. Chem. Soc.* **2009**, *131*, 3611.
[49] Gaussian 09, Revision **A.1**, M. J. Frisch, G. W. Trucks, H. B. Schlegel, G. E. Scuseria, M. A. Robb, J. R. Cheeseman, G. Scalmani, V. Barone, B. Mennucci, G. A. Petersson, H. Nakatsuji, M. Caricato, X. Li, H. P. Hratchian, A. F. Izmaylov, J. Bloino, G. Zheng, J. L. Sonnenberg, M. Hada, M. Ehara, K. Toyota, R. Fukuda, J. Hasegawa, M. Ishida, T. Nakajima, Y. Honda, O. Kitao, H. Nakai, T. Vreven Jr., J. A. Montgomery, J. E. Peralta, F. Ogliaro, M. Bearpark, J. J. Heyd, E. Brothers, K. N. Kudin, V. N. Staroverov, R. Kobayashi, J. Normand, K. Raghavachari, A. Rendell, J. C. Burant, S. S. Iyengar, J. Tomasi, M. Cossi, N. Rega, J. M. Millam, M. Klene, J. E. Knox, J. B. Cross, V. Bakken, C. Adamo, J. Jaramillo, R. Gomperts, R. E. Stratmann, O. Yazyev, A. J. Austin, R. Cammi, C. Pomelli, J. W. Ochterski, R. L. Martin, K. Morokuma, V. G. Zakrzewski, G. A. Voth, P. Salvador, J. J. Dannenberg, S. Dapprich, A. D. Daniels, Ö. Farkas, J. B. Foresman, J. V. Ortiz, J. Cioslowski, D. J Fox, Gaussian, Inc., Wallingford CT, **2009**.
[50] Y. Zhao, D. G. Truhlar, *Theor. Chem. Acc.* **2008**, *120*, 215.
[51] A. K. Rappe, C. J. Casewit, K. S. Colwell, W. A. Goddard III, W. M. Skiff, *J. Am. Chem. Soc.* **1992**, *114*, 10024.
[52] V. A. Rassolov, J. A. Pople, M. A. Ratner, T. L. Windus, *J. Chem. Phys.* **1998**, *109*,1223.
[53] T. Vreven, B. Mennucci, C. O. da Silva, K. Morokuma, J. Tomasi, *J. Chem. Phys.* **2001**, *115*, 62.